Journal of Data Acquisition and Processing
ISSN: 1004-9037
https://sjcjycl.cn/
DOI: 10.5281/zenodo.754723

AN EFFICIENT SECURED LS AUTHENTICATION SYSTEM THROUGH FREQUENT PATTERN-GROWTH (FP-GROWTH) TECHNIQUE

[1]Dr. A. Devi, [2]Ms. R. Lavanya, [3]Mr. T. Kumersan.
[1]Associate Professor, Department of Computer Applications, Dr. SNS Rajalakshmi College of Arts & Science, Coimbatore.
[2]PG Student, II MCA, Department of Computer Applications, Dr. SNS Rajalakshmi College of Arts & Science, Coimbatore.
[3]PG Student, II MCA, Department of Computer Applications, Dr. SNS Rajalakshmi College of Arts & Science, Coimbatore.

Abstract: - Laser speckle has been planned in a very variety of works as a high-entropy supply of unpredictable bits to be used in security applications. Bit strings derived from speckle may be used for a range of security functions like identification, authentication, anti-counterfeiting, secure key storage, random variety generation and tamper protection. The selection of laser speckle as a supply of random keys is kind of natural, given the chaotic properties of speckle. This work proposes an optical device speckle recognition system for credibility verification. Owing to the distinctive state surfaces of objects, laser speckle provides diagnosable features for authentication. A Gabor filter, SIFT (Scale-Invariant Feature Transform), and projection were wont to extract the features of optical device speckle images. To accelerate the matching method, the extracted Gabor features were organized into an indexing structure using the modified K-means algorithm. The special relations among the matching points are then remodeled to 9DLT (Direction Lower Triangular) representations. Then, the Frequent Pattern Growth (FP-Growth) algorithm mines frequent patterns therefore a helpful association rule is obtained because the feature to spot the similarity between every of the speckle pictures for the aim of credibility verification. Plastic cards were used because the target objects within the planned system and also the hardware of the speckle capturing system was designed. The experimental results showed that the retrieval performance of the planned methodology is correct once the information contains 516 optical device speckle pictures. The planned system is powerful and possible for credibility verification.

Keywords: Image Processing, Imaging Systems, Pattern Recognition, Optical Security and Encryption, K-means algorithm, FP-Growth algorithm, Direction Lower Triangular.

1. INTRODUCTION

Because of an increasing emphasis on personal privacy, security, and convenience, authenticity verification systems are a crucial issue in academic and industrial fields. To ensure that only legitimate users have access, the systems of service providers require secure and reliable schemes to effectively identify the individual requesting the services. Possible applications include secure access to buildings, entrance guards, computer systems, and ATMs. Although transitional magnetic and IC cards can achieve this purpose, they can be easily duplicated using current technology [1, 2]. Therefore, the development of other objects that contain a unique physical identity code to secure access is vital. Optical technology is used in

data security and identity verification [3, 4] to solve the duplication issue of transitional magnetic and IC cards. It has the advantage of no RF interference from nearby objects and is more secure because of the highly directional property of optical communication.

Data encryption technology is also used to provide an additional layer of security. However, the disadvantage of optical identification is environmental factors, such as fog, rain, and the lack of line of sight information. Biometric recognition [5], also called biometrics, has received considerable attention for security access applications in the past decade. Biometrics uses body characteristics, such as fingerprints, faces, irises, and voices. Fingerprint recognition [6, 7] is one of the oldest methods to recognize or verify people, because each person has a unique fingerprint structure that consists of ridges and valleys. Face recognition [8, 9] techniques identify faces by extracting facial features, such as the relative position, size, eyes, lips, nose, jaw, and cheekbones.

The iris region contains visual texture, which carries distinctive information that is useful for personal identification [10, 11]. Biometrics techniques use the body of a person as a key; therefore, it is unnecessary to purchase a passport, smart card, ID card, or key. Each body part has a unique identity to achieve personal identification. However, biometrics requires numerous data to be stored for a person, and these types of systems are not always reliable because humans change over time. In addition, biometrics is expensive and the design of such systems is complex. The speckle effect is observed when coherent light is scattered from a rough surface. If the surface is sufficiently rough to create path length differences, the intensity of the resultant light varies randomly.

2. PROPOSED LASER SPECKLE IDENTIFICATION SYSTEM

2.1. Speckle Capturing Device Development

The proposed laser speckle capturing device is shown in Fig. 2.1. The dimensions of the device is 300 100 200 mm (length width height). The capturing device consists of a CCD (Charge-Coupled Device) camera equipped with an aperture and lens to record the reflected laser speckle pattern from the plastic cards, as shown in Fig. 3.1. A laser diode was used to generate a highly coherent light, as shown in Fig. 4(b). The wavelength of the laser was 635 nm and the resolution of the image sensor was 480 640 pixels with a pixel size 8.3 um 8.3 um. The actual coverage area of the plastic cards captured from the image sensor was approximately 4687 um 6249 um, because the magnification ratio of the speckle capturing device was 0.85 (4687 um = 480 × 8.3 um × 1 0.85, 6249 um = 640 × 8.3 um × 1 0.85)

Fig. 2.1: - The prototype of the proposed laser speckle is capturing device (a) appearance, (b) interior, and (c) bird's eye view with blue plastic card.

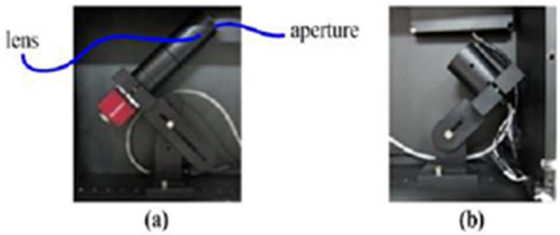

Fig. 2.2: - Components of the capturing device (a) digital camera and (b) laser source.

The angles between the capturing device and the card surface and that between the laser diode and the card surface are notated as and θ, respectively. The angle is in the range of θ+10º <= < 90º. In our prototype, we select f as 45º and θ as 30º. The plastic card illustrated by a highly coherent light emitted from a laser diode resulted in scattered lights from the card surface. The scattered lights subsequently pass through the aperture and lens in front of the image sensor, resulting in a diffractive effect. The diffractive effect produces several bright spots, which interfere with each other. These bright spots generate a distribution of bright and dark spots by constructive and destructive interference, respectively. Therefore, the distribution of the bright and dark spots forms a speckle pattern on the image sensor and is invariant after slight displacement.

2.2 Feature Extraction for Speckle Recognition

Feature extraction is that the method of spatial property reduction within which the input file is reworked into a reduced illustration set of features (also referred to as feature vectors). Therefore, the chosen features should with efficiency represent the initial knowledge for recognition functions. In our projected recognition system, a physicist filter, SIFT, and projection processes were accustomed extract features from the captured laser speckles. These features sets extract relevant data from laser speckles for identification exploitation reduced illustration rather than the complete size knowledge.

2.3. Gabor Filter Features

In image process, Gabor filters have frequency and orientation representations of the image, which is comparable to those of the human sensory system. Gabor filters are acceptable for texture illustration and discrimination. Here, introduced 2-D Gabor wavelets over the image domain for iris recognition. The Gabor wavelets (GWs) composed of a 2-D Gaussian function and complicated function are an image process tool that has been wide utilized in image decomposition and illustration. The Gabor wavelets is outlined as follows

$$\Psi_{\mu,\nu}(z) = \frac{\|\vec{k}_{\mu,\nu}\|^2}{\sigma^2} e^{-\frac{\|\vec{k}_{\mu,\nu}\|^2 \|z\|^2}{2\sigma^2}} \left[e^{i\vec{k}_{\mu,\nu} z} - e^{-\frac{\sigma^2}{2}} \right]$$

Where μ and ν is the orientation and scale of the GWs, is the point of the original image with horizontal coordinate x and vertical coordinate y, indicates the norm operator, and s is related to the standard deviation of the Gaussian window and determines the ratio of the Gaussian window width to the wave length. is the wave vector and is defined as follows:

$$\vec{k}_{\mu,v} = \vec{k}_v e^{i\varphi_\mu}$$
$$\varphi_\mu = \frac{\mu\pi}{8} \text{ for } \mu \in \{0,1,\ldots 7\}$$
$$k_v = k_{max}/f^v \text{ for } v \in \{1,2,3,4\}$$

where is the maximal frequency and is the spatial frequency between kernels in the frequency domain. A Gabor function with eight orientations (i.e., μ ∈{0,…7}) and five scales (i.e.,v ∈{0,…,4}) were used to generate the Gabor wavelets [12]. The Gabor feature illustration of 40 images was generated by convolving a laser speckle image with every of the Gabor wavelets. In an exceedingly physicist feature illustration of the image, every pixel value within the grey level is accumulated, and therefore the accumulated results of forty images are concatenated to make a 40-dimentional feature vector. When the accumulating method, the compressed Gabor features were incorporated in database clustering to accelerate feature matching. The Figure 5 represents the real part of the Gabor wavelets with five scales and eight orientations.

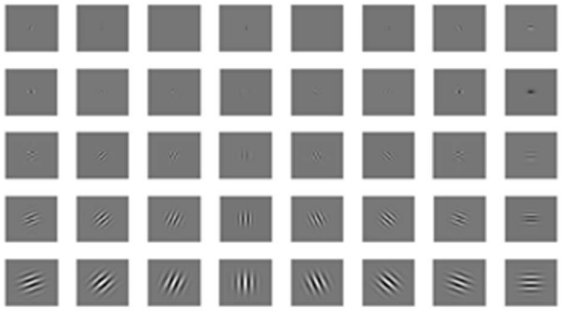

Fig. 2.3: - Real part of the Gabor wavelets with five scales and eight orientations.

3. SIFT FEATURES

SIFT (Scale Invariant Feature Transform), projected [13], and may be a powerful tool for extracting distinctive invariant features from images and may be accustomed perform reliable matching between differing views of an object or scene [14]. Hence, SIFT is applied in numerous fields involving video trailing, navigation, and recognition [15]. The primary step of SIFT is key-point detection. An input image is convolved with Gaussian functions at numerous scales. Key-points are after used as maxima/minima of the distinction of Gaussians (DoG) and occur at multiple scales k. Thus, the locations of the key-points are obtained by detection the maxima and minima of DoG images. After, the unstable key-points are discarded, like low-contrast or the placement at the sting. The Taylor enlargement and hessian matrix were accustomed eliminate unstable key-points. To realize invariableness to rotation, every stable key-point is assigned one or additional orientations supported native image gradient directions. The key-point is delineated relative to the precise orientation to be invariant to image rotation. Finally, every key-point is delineated supported a patch of pixels in its native neighborhood. Figure seven shows SIFT key-point descriptor of the laser speckle images. within the left side of Fig. 3.1, the arrows in an exceedingly eight × eight set of samples represent the gradient magnitude and orientation computed at every sample in an exceedingly region around the key-point location. The circular window represents a Gaussian function accustomed assign a weight

to the magnitude of every sample purpose. The samples in each 4 × 4 sub regions are accumulated into eight directions orientation histogram to form a 2 × 2 descriptor array. The length of each arrow corresponds to the magnitudes of the accumulated gradient within the sub region. Figure 6 shows the feature points extracted by SIFT.

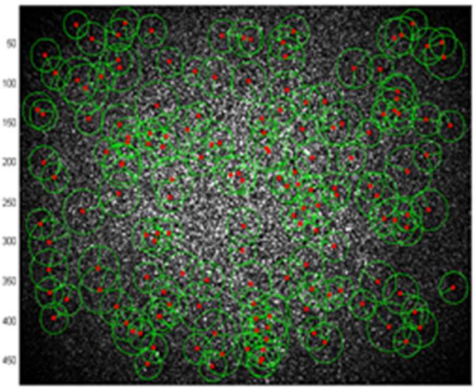

Fig. 3.1: -. SIFT key-points of the laser speckle images

4. PROJECTION FEATURES

The matching of SIFT key-points may encounter a problem in which two speckles differ but have a similar number of key-points. In such a scenario, the SIFT cannot determine the most similar speckle. The projection features shown in Fig. 4.1, were used to solve this problem. The speckles were projected to x and y axes to obtain the features shown in Fig. 4.1(b) and Fig. 4.1(c), respectively.

$$r = \frac{\sum_i (A_i - \bar{A})(B_i - \bar{B})}{\sqrt{\sum_i (A_i - \bar{A})^2 (B_i - \bar{B})^2}}$$

After calculating the correlation of concatenated x and y projection features, we selected the speckle with the highest correlation. Finally, the speckle was verified by a threshold; the speckle must pass the predefined threshold to be regarded as a recognition result.

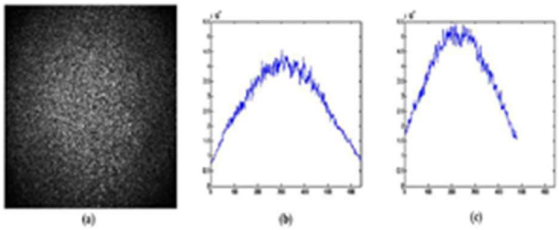

Fig. 4.1: - Projection features (a) original speckle image (b) projection along x-axis, and (c) projection along y-axis.

Database Organization

The planned system is also applied to attendance signatures and may accommodate a considerable user flow throughout an exact amount of time. Therefore, the system should method an outsized quantity of information in real time. Efficient database organization is crucial for increasing the feasibleness of the system. A coarse-to-fine strategy is appropriate

for matching the target speckle within the information set in real time environments with time constraints. Within the opening move, the modified K-means algorithm [16] was used to organize the Gabor filter features into an assortment structure. If the information is clustered into n teams, the matching method is merely performed on the cluster within which the representative feature vector is a lot of almost like that of the target feature vector. Therefore, the matching time may be reduced significantly. Afterwards, the candidate speckles within the chosen cluster are verified by SIFT to spot whether or not these candidates don't have any record within the information. Finally, the project features are used to choose the feature that's most almost like the target speckle captured from the system.

Spatial relations establishment through 9DLT

Many researchers are planned to seek out the association rules of spatial relations among objects in a picture. Hsu et al. initial planned the point of view mining technique in 2003. However, the spatial relation illustration of the point of view mining technique planned by Hsu et al., that considers each the pixel distance and angular unit between objects, is simply too advanced to explain the similarity of the spatial relations of the matching points. And additionally planned a symbolic assortment approach referred to as "9DLT matrix" to encode symbolic pictures and preserve the spatial relations among objects. we discover that Chang's technique is a lot of intuitive in addressing the relative positions of matching points than absolutely the locations of Hsu et al.'s technique as a result of the speckle images usually have slight variations once the photographs are captured at totally different time slots via a optical maser capturing device.

FP-Growth Algorithm in Association Rules Mining 9DLT string is a series of symbols that indicate the matching points and their spatial relations. For each plastic card, we extract its M speckle images and select 1 as a basis for finding the matching points of . Then, the Fp-Growth with Apriori algorithm is used to find the frequent patterns or the so-called association rules. An association rule states that when X occurs, Y occurs with a certain probability. Association rule mining problem could be stated by the following definitions.

Definition 1: Let $F = \{f_1, f_2, \dots, f_M\}$ be a set of images captured from the same cards.

Definition 2: A representative image f_b is used to calculate the matching points of other *M*-1 images denoted as $F' = \{f_t | f_t \in F\{f_b\}\}$

Definition 3: Let $V = \{v_1, v_2, \dots, v_l\}$ be a set of l distinct matching points, and $Z = \{z_1, z_2, \dots, z_l\}$ indicates the ordered matching points of *V* called "the items".

Definition 4: The spatial relation between two matching points is 1 of the 9 directions defined by 9DLT representation. The 9DLT representation of the matching point set is a pattern $A = \{a_1, a_2, \dots, a_l, ra_1, ra_2, \dots, ra_h\}$, where a_i is an item, ra_j is a spatial relation of the item. Here, the spatial relations between any two items are recorded in this pattern. A pattern with *l* items is named the *l* -pattern. Note that there is no spatial relation for the pattern of length 1.

Definition 5. Each speckle image of F' will produce an *l*-pattern 9DLT string, and each of the strings is regarded as 1 transaction.

Definition 6. The *support* of a pattern is defined as the percentage of transactions that contains the pattern. A pattern is called "frequent itemset" if its support is no less than a predefined threshold, α_{min-s} . The frequent itemset are identified using Fp-Growth [17].

Here, we have *M l*-patterns for each registered plastic card and the Apriori algorithm is applied to identify the association rules whose minimum support is larger than the predefined

threshold,$\alpha_{min-sup}$. Our method evaluates important association rules for all registered plastic cards in the entire database.

Identification process

During the identification process, the CCD camera captures the laser speckle image of the target plastic card to be identified. To accelerate the matching process, we suggest a method that measures the similarity between the two speckles through their matching association rules in the following equation:

$$f_{score}^{\tau} = \sum_{l=\sigma+1}^{L}(1-\sigma) \times \frac{|M_l^{\tau}|}{|S_l^{\tau}|} 2 \leq l < -L, \tau = 1,2, \dots N$$

where |.| denotes the size of a set, $|S_l^{\tau}|$ represents the set of the association rules with size l in the τ -th card, M_l^{τ} represents the matched rules between the test card and the τ -th card with size l, represents the length of the items of the association rules, τ is the largest set of S_l^{τ} , and L is the length of the longest itemset of the association rule.

Subsequently, all speckle images in the selected group were fed to the SIFT feature matching process to compares their key-points with that of the target speckle (the acquired laser speckle image). In the SIFT matching process, the speckle that has the most matching key-points is the final recognition result. When two or more speckles have the same number of key-points, the correlation of the project feature between each of these speckles and the target speckle is used to select the optimal match that has the largest correlation value [18]. If the key-points of all speckles in the selected group are lower than a predefined threshold, the target speckle is identified as the unregistered item.

5. EXPERIMENTAL RESULTS

A total of 50 numbered plastic cards created from a complete of four totally different styles of materials are used to check the performance of the projected recognition system. Once the light beam indicates the rough surface of a plastic card, the reflected light is scattered all told directions, the CCD captures the reflected light, and therefore the speckle pattern of the check card is detected within the image plane. every card is captured ten times; thus, we have a tendency to acquire a complete of five hundred laser speckle pictures to coach the association rules with p=500, α =2.3, and support = 0.75. Two extra plastic cards are used for testing new things not registered in our database.

Accuracy Comparison: -

As shown in Fig. 5.1, accuracy of the proposed method achieves higher classification accuracy than the existing method and the accuracy result is illustrated in Figure 5.1, since in proposed work perform FP-Growth offered in order to reduce the errors.

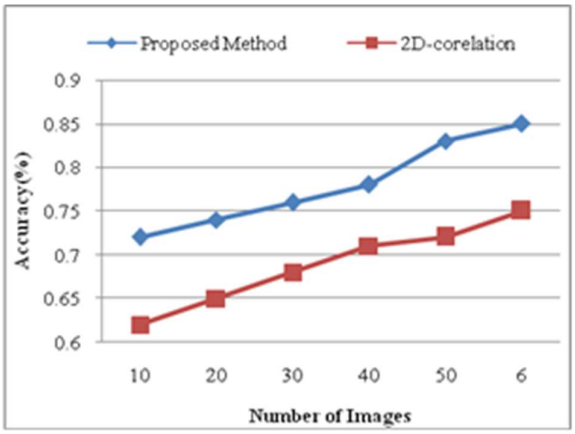

Fig. 5.1: -. Accuracy Comparison

Computational Time comparison

As shown in Fig. 5.2, computation time of the proposed method is lower than the existing method and the computation time is illustrated in Figure 5.2, since in proposed work perform FP-Growth offered in order to produce the frequent patterns.

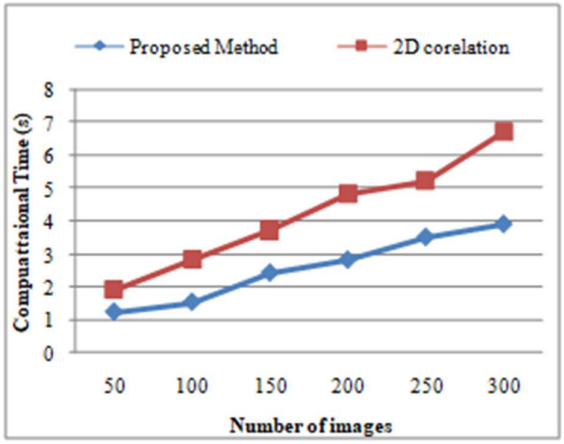

Fig.5.2: -. Computational Time Comparison

6. CONCLUSION

This work proposed a laser speckle recognition system for authenticity verification. Here, to build an image to capture the laser speckles of plastic cards. Many options, as well as a Gabor filter, SIFT, and projection was extracted from laser speckles against the changes of speckles caused from a small displacement of cards once capturing. The indexing structure was designed for the info to accelerate the matching method. The experimental results show that the projected device will capture the laser speckles of plastic cards, and therefore the recognition technique has high identification accuracy. The projected technique exhibits superior performance to it of Buchanan et al. (2D-coorelation) concerning identification accuracy and time. within the close to future, we are going to implement our technique on the embedding system to scale back the specified time of identification and check alternative materials, like paper, to increase the vary of applications of the laser speckles for legitimacy verification.

REFERENCES

[1] Keilbach, P., Kolberg, J., Gomez-Barrero, M., Busch, C., & Langweg, H. (2018, September). Fingerprint presentation attack detection using laser speckle contrast imaging. In 2018 international conference of the biometrics special interest group (BIOSIG) (pp. 1-6). IEEE.

[2] Mirzaalian, H., Hussein, M., & Abd-Almageed, W. (2019, June). On the effectiveness of laser speckle contrast imaging and deep neural networks for detecting known and unknown fingerprint presentation attacks. In 2019 International Conference on Biometrics (ICB) (pp. 1-8). IEEE.

[3] Shaydyuk, N. K., & Cleland, T. (2016, October). Biometric identification via retina scanning with liveness detection using speckle contrast imaging. In 2016 IEEE International Carnahan Conference on Security Technology (ICCST) (pp. 1-5). IEEE.

[4] Sun, C., Jagannathan, A., Habif, J. L., Hussein, M., Spinoulas, L., & Abd-Almageed, W. (2019, May). Quantitative laser speckle contrast imaging for presentation attack detection in biometric authentication systems. In Smart Biomedical and Physiological Sensor Technology XVI (Vol. 11020, pp. 38-46). SPIE.

[5] Blau, Y., Bar-On, O., Hanein, Y., Boag, A., & Scheuer, J. (2020). Meta-hologram-based authentication scheme employing a speckle pattern fingerprint. Optics Express, 28(6), 8924-8936.

[6] van Welzen, J., Yuan, F. G., & Fong, R. Y. (2022). Hidden damage visualization using laser speckle photometry. NDT & E International, 131, 102700.

[7] van Welzen, J., Yuan, F. G., & Fong, R. Y. (2021, March). Comparison of image correlation algorithms for hidden damage laser speckle photometry. In Sensors and Smart Structures Technologies for Civil, Mechanical, and Aerospace Systems 2021 (Vol. 11591, pp. 132-151). SPIE.

[8] Yeh, C. H., Lee, G., & Lin, C. Y. (2015). Robust laser speckle authentication system through data mining techniques. IEEE Transactions on Industrial Informatics, 11(2), 505-512.

[9] Sjödahl, M., & Olsson, E. (2021). Robustness of Laser Speckles as Unique Traceable Markers of Metal Components. Digital, 1(1), 54-63.

[10] Zhao, Q., Li, H., Yu, Z., Woo, C. M., Zhong, T., Cheng, S., ... & Lai, P. (2022). Speckle-Based Optical Cryptosystem and its Application for Human Face Recognition via Deep Learning. Advanced Science, 9(25), 2202407.

[11] Cester, L., Starshynov, I., Jones, Y., Pellicori, P., Cleland, J. G., & Faccio, D. (2022). Remote laser-speckle sensing of heart sounds for health assessment and biometric identification. Biomedical Optics Express, 13(7), 3743-3750.

[12] Kalyzhner, Z., Levitas, O., Kalichman, F., Jacobson, R., & Zalevsky, Z. (2019). Photonic human identification based on deep learning of back scattered laser speckle patterns. Optics Express, 27(24), 36002-36010.

[13] Smolovich, A. M., Frolov, A. V., Klebanov, L. D., Laktaev, I. D., Orlov, A. P., Smolovich, P. A., & Butov, O. V. (2024). Identification of a replicable optical security element using laser speckle. Optics & Laser Technology, 175, 110725.

[14] Ryckewaert, M., Héran, D., Faur, E., George, P., Grèzes-Besset, B., Chazallet, F., ... & Bendoula, R. (2020). A new optical sensor based on laser speckle and chemometrics for precision agriculture: application to sunflower plant-breeding. Sensors, 20(16), 4652.

[15] Guarnera, F., Allegra, D., Giudice, O., Stanco, F., & Battiato, S. (2019, September). A new study on wood fibers textures: documents authentication through LBP fingerprint. In 2019 IEEE International Conference on Image Processing (ICIP) (pp. 4594-4598). IEEE.

[16] Schwarz, A., Shemer, A., Ozana, N., García, J., & Zalevsky, Z. (2017, May). An optical remote sensor for fingerprint identification using speckle pattern. In 2017 Conference on Lasers and Electro-Optics (CLEO) (pp. 1-2). IEEE.

[17] Blau, Y., Bar-On, O., Kotlicki, O., Hanein, Y., Boag, A., & Scheuer, J. (2018, July). Holographic anti-counterfeiting tags utilizing speckle pattern "fingerprint". In Novel Optical Materials and Applications (pp. NoW1D-1). Optica Publishing Group.

[18] van Welzen, J., Yuan, F. G., & Fong, R. Y. (2021, March). Comparison of image correlation algorithms for hidden damage laser speckle photometry. In Sensors and Smart Structures Technologies for Civil, Mechanical, and Aerospace Systems 2021 (Vol. 11591, pp. 132-151). SPIE.